Journal of Microelectronics and Electronic Packaging (2013) **10**, 73-79

ISSN: 1551-4897

The Distribution and Transport of Alpha Activity in Tin

Brett M. Clark*

Abstract—**The presence of alpha emitters in packaging materials poses an increased risk to device reliability as device size decreases and flip chip and 3D packaging technology becomes more widespread. Particularly troubling is the observation that alpha emission increases over time in some reported instances. Several experiments were conducted to examine alpha flux behavior in tin materials and determine the cause for the temporal alpha emissivity increase. The experiments determined the distribution of the alpha emitters within the material volume, and a mechanism based on microsegregation is presented to explain the nonuniform distribution. Data describing differential isotope distribution within tin are also presented, providing confirmation of ^{210}Po transport within a solid tin matrix. The effects of microsegregation and ^{210}Po migration on alpha emissivity over time are discussed. Potential impacts from these mechanisms on alpha emissivity in packaging applications are presented.**

Keywords—**Alpha emissivity, microsegregation, polonium diffusion, soft errors**

Introduction

The issue of soft error reliability and the contribution of alpha emitting isotopes to single-event upsets (SEUs) have been studied over the past decade [1, 2]. Initial research focused on Pb-based solders used in semiconductor packaging and efforts to improve purity, particular with respect to alpha emitting isotopes [3]. The transition to Pb-free materials has shifted focus to tin-based materials. In general, radioactivity decreases over time in materials not exposed to nuclear reactor conditions. However, several examples where alpha emission increases significantly have been observed in lead-based materials [3, 4]. Alpha emissivity increasing over time increases SEU risk in devices sensitive to alpha induced upsets [4]. Furthermore, the proximity of emitters with respect to a sensitive node can have a significant impact on SEUs.

Alpha emitting isotopes are present in the packaging materials at parts per billion concentrations and below [5]. This paper will focus on the contribution of these trace elements, particularly the uranium decay chain daughter ^{210}Po. One common explanation for increasing alpha emissivity revolves around the disturbance of ^{210}Pb/^{210}Po secular equilibrium, and subsequent reestablishment of secular equilibrium with a resultant increase in alpha flux [6]. Some experimental data reported for Pb materials follows this mechanism [4], while other reported data departs from the behavior predicted [3]. No comparable time-dependent alpha emissivity data has been reported for tin materials. With Sn-based materials becoming the preferred alternative to Pb, determining the temporal alpha emission characteristics of Sn is necessary. Several experiments were carried out to assess distribution of alpha emitters in Sn and to describe the factors influencing the time dependence of the observed alpha emissivity. This paper presents data describing changing alpha emissivity in tin and reports a combination of mechanisms where alpha emission in a material may increase over time. Data presented demonstrate that alpha emitting isotopes are not uniformly and randomly distributed. We propose mechanisms for nonuniform distribution and alpha emissivity data characterizing the nonuniformity.

The manuscript was received on January 21, 2013; revised on April 3, 2013; accepted on June 4, 2013

Honeywell Electronic Materials, Spokane, Washington 99216
*Corresponding author; email: Brett.Clark@Honeywell.com

Experiments

A. Experiment 1: Characterization of Microsegregation

Two experiments were performed to assess activity distribution in 99.99% pure tin used for lead-free solders. The first experiment involved three different tin samples. The three samples were chosen on the basis of differential increasing alpha emission rate. As displayed in Fig. 1, Sample A showed no significant increase in alpha emissivity within measurement uncertainty over a period of two years, while samples B and C showed increasing counts within several months of processing.

The sheets were etched in 70% by volume high purity distilled hydrochloric acid/30% CMOS grade nitric acid to remove surface material, and washed thoroughly with deionized water. Sheets were weighed before and after etching, and the depth of tin removed was calculated assuming uniform dissolution from the surface. The final sample thickness agreed with the calculated value assuming initial thickness less the etched material. Alpha flux measurements were performed using an Alpha Sciences 1950 gas proportional counter. Measurement protocols followed those recommended in JESD221 [7]. Multiple iterations of the procedure were done, measuring the alpha activity at each successive surface. The range of a 5.3 MeV alpha particle in Sn is 16.5 μm [8], and at least this material depth was etched away at each step to remove the previous analytical volume.

B. Results and Discussion

The alpha emissivity versus the first 100 μm in depth is plotted in Fig. 2. Sample A shows no significant change, while samples B and C show significant increase. The increase is strongly linear versus depth within the initial 100 μm, with correlation coefficients of 0.98 and 0.99. The strong correlation across multiple samples suggests that the experimental

doi:10.4071/imaps.361

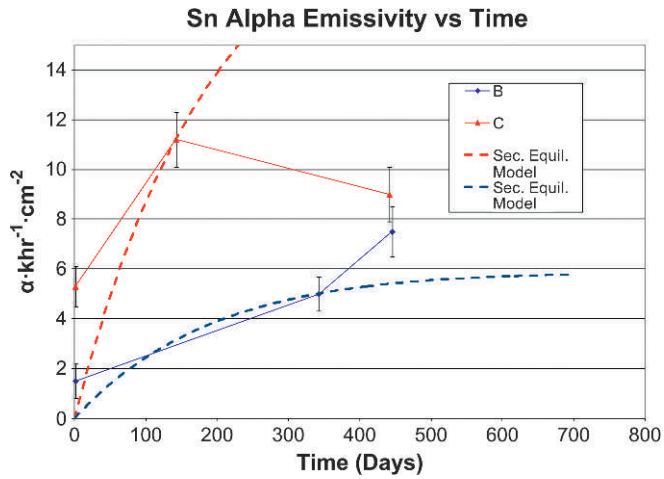

Fig. 1. Alpha flux versus time for three Sn samples. Error bars show 1 σ error.

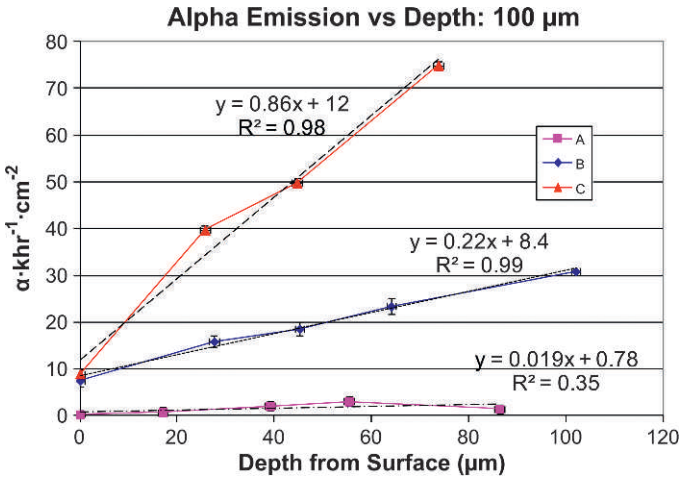

Fig. 2. Alpha emission versus 100 µm depth in three Sn samples.

protocol did not introduce significant variation with respect to alpha emitter contaminants. The emissivity increase versus depth scales with the differential surface alpha emissivity, namely $\Delta\alpha_C > \Delta\alpha_B > \Delta\alpha_A \approx 0$. These data suggest the emitter concentration gradient in the material is directly proportional to the surface alpha emissivity increase on the surface. The surface alpha emissivity for sample B increased by a factor a 5 over 15 mo, while sample C emissivity doubled.

The expected alpha emissivity versus time due to secular equilibrium is plotted in Fig. 1 for samples B and C. These curves were generated by calculating the number of ^{210}Pb atoms per cm^2 needed to increase the alpha flux in the respective samples to the initial data points in the requisite time. Both samples B and C deviate significantly from secular equilibrium predictions, and an additional time-dependent mechanism is required to explain the data.

The distribution of alpha emitters within the material volume is explained by microsegregation, a well documented metallurgical phenomenon [9]. Microsegregation arises in solid/liquid systems where solutes (e.g., alpha emitting isotopes) partition preferentially in the liquid phase versus the solid phase during solidification according to

$$k = \frac{C_S}{C_L} \tag{1}$$

where k is defined as the partition coefficient, and C_S and C_L are the concentrations in the liquid and solid phases, respectively. As solidification fronts propagate, solute concentration in the liquid phase increases if $k < 1$. The result is an elemental gradient along the solidification axis, with the largest solute concentration located in the final solidification volume. The gradient slope is a function of solidification rate and the solute concentration. Microsegregation is commonly observed in commercial alloys [10]. One common technique employed to minimize microsegregation is rapid solidification. It should be noted that all three samples experienced comparable solidification conditions.

The different depth profiles of samples A, B, and C may be explained in terms of the concentration of alpha emitters within each. The higher the emitter concentration in the liquid phase, the larger the amount that partitions during solidification at each point within the depth according to eq. (1), and the steeper the gradient. The ^{210}Po concentration equivalent to a measured alpha flux $\varepsilon_{measured}$ may be calculated from

$$[Po_\alpha](ng/g) = \frac{10^9 \varepsilon_{measured} M}{\lambda N_A \rho A R f} \tag{2}$$

where λ is the decay reaction rate constant in hours, N_A is Avogadro's number, ρ is the density of the matrix in grams per mole, A is the measurement area in cm^2, R is the alpha range in the matrix in centimeters (16 µm for the 5.3 MeV alpha), M is the molar mass of the emitter, and f is a geometric correction factor [3]. Fig. 3 shows the projected alpha emission as a function of polonium concentration assuming all the emission originates from polonium. The maximum value of sample C in Fig. 2 (74.9 $\alpha \cdot kh^{-1} \cdot cm^{-2}$) corresponds to 1.5×10^{-18} g of ^{210}Po per gram of Sn, or 4.2×10^3 ^{210}Po atoms per gram of Sn. The data suggest solute microsegregation is present several orders of magnitude below the parts per billion (ppb) concentration range previously proposed for trace contamination [5].

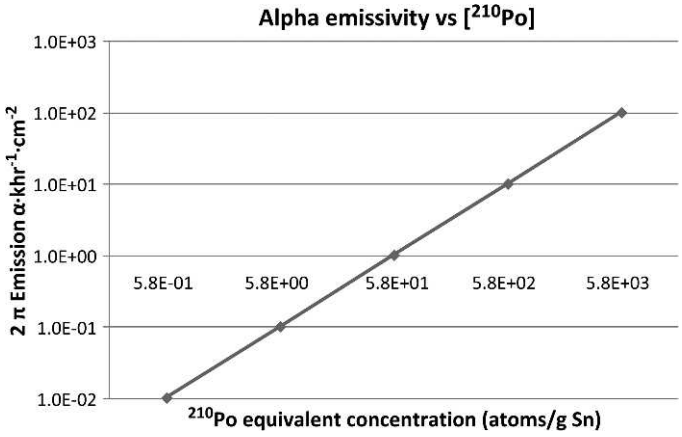

Fig. 3. Theoretical alpha emissivity versus ^{210}Po concentration.

While direct measurement of impurity concentration would be helpful, the analytical levels required are below current measurement capability. Glow discharge mass spectrometry (GDMS) analysis of tin failed to detect alpha emitting contaminants above 0.5 ppb detection limits. We therefore infer concentration changes from alpha radiation measurements.

The time dependence of alpha emissivity in Sn deviates from what is predicted by secular equilibrium. Nevertheless, the correlation between the concentration of impurities sequestered inside the material and the emissivity change over time suggests that a secondary mechanism is active.

C. Experiment 2

A second experiment examined the alpha emitter distribution in an Sn ingot. The center portion of an ingot was removed and reduced to 0.81 mm thick. The initial area of 900 cm^2 had an alpha emissivity of 18.4 $\alpha \cdot kh^{-1} \cdot cm^{-2}$. The analytical volume of the measurement was 1.5 cm^3, which represents only 0.1% of the sample volume. After initial measurement, the sample was rolled to progressively thinner dimensions and measured at each thickness. Metal temperature did not exceed 303 K during the reduction processes. Both sides of the sample were measured to increase the effective volume at each iteration. Measurements were conducted using a XIA Ultra-Lo 1800 ionization chamber, which has previously been used to study alpha emissivity [11]. The larger active area of this instrument enabled a greater volume of material to be analyzed, and the energy spectra generated enabled identification of the specific alpha emitting isotopes.

D. Results and Discussion

Table I contains the experimental parameters and the corresponding alpha emissivity data. The results show alpha emissivity increasing with decreasing sample thickness. These data are consistent with the observation in the previous experiment: that surface emissivity measurements significantly underestimate the thick sample emissivity where microsegregation effects are present. In addition, the emissivity from side A is statistically different from side B. This may indicate that one surface is closer to the final solidification zone than the other.

The alpha spectrum was measured for both thick and thin samples and normalized to counting time. Differences in the alpha emission spectra (Fig. 4) for sample thickness were observed. Sample A (thick) exhibited a pronounced surface ^{210}Po peak similar to surface emission from Sn solder bumps reported by Gordon [4]. Sample D (thin) lacks prominent ^{210}Po emission but exhibits more emission in the 1-4.5 MeV range.

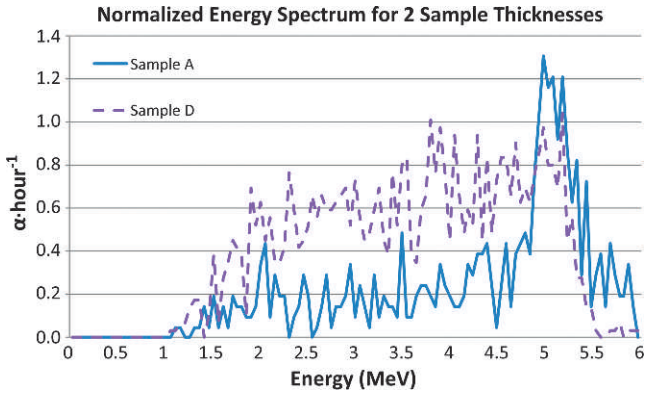

Fig. 4. Energy spectra comparison.

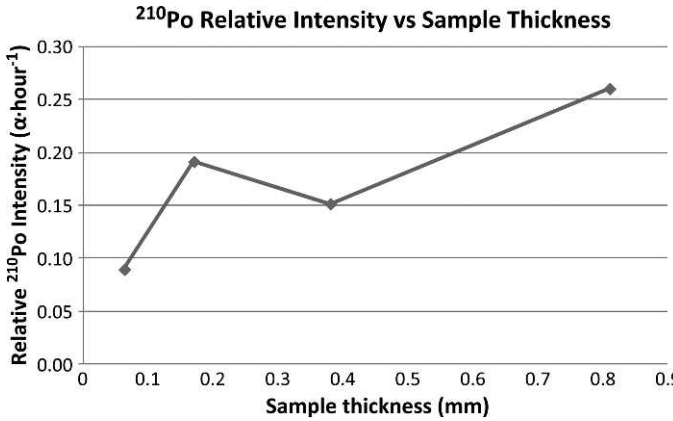

Fig. 5. ^{210}Po relative surface emission versus sample thickness.

This characteristic suggests that the emitting species are more concentrated subsurface than in the 0.81 thickness.

The ^{210}Po surface emissivity (5.1-5.6 MeV) relative to the total integrated counts from 1-8.5 MeV for different thicknesses is plotted in Fig. 5. For the 0.81 mm sample, ^{210}Po surface emission constitutes greater than 20% of the detected emissivity. The percentage hovers between 15 and 20% for intermediate thickness samples before dropping to less than 10% of the detected emissivity in 0.063 mm thick samples. The bulk activity increases by factor of two from the surface to the interior, but the ^{210}Po component decreases by a comparable factor. The broad spectrum below 5.3 MeV for sample D is consistent with subsurface ^{210}Po alpha emission, wherein a fraction of the energy is lost via interaction with the matrix prior to exit. These data support the hypothesis that ^{210}Po is nonuniformly distributed due to microsegregation in the ingot.

Table I
Data for Alpha Emissivity versus Tin Volume Analyzed

Sample thickness	Thickness (mm)	Sample area (cm^2)	Percent of volume analyzed (both surfaces)	Bulk alpha emissivity ($\alpha \cdot cm^{-2} \cdot kh^{-1}$)			
				Side A	1 σ	Side B	1 σ
A	0.81	1,800	4	17.2	0.7	14.8	0.6
B	0.38	1,800	9	30.2	0.9	29.1	0.7
C	0.17	1,800	19	36.1	0.9	32.4	0.9
D	0.063	1,800	54	32.9	0.7	28.8	0.5

The experimental data presented above demonstrate that alpha emitting isotopes are not randomly distributed in the material undergoing liquid/solid phase transition. This hypothesis was earlier proposed by Clark [3]. Typical metal manufacturing processes involve melting and solidification steps, during which alpha emitters may be concentrated in the interior of the mass. Test samples made from solidification processes are expected to experience microsegregation effects. Alpha emissivity measurements conducted on samples thicker than the alpha escape range will yield an emissivity lower than the value for the entire volume when this mechanism is operable.

Experiment 3: Characterization of Diffusion

The observation of consistent ^{210}Po surface emission warranted further investigation to identify the source of this activity. ^{210}Po is a ^{222}Rn daughter, and atmospheric ^{222}Rn has been proposed as a potential polonium source [6]. An alternative explanation was proposed by Zastawny, who reported polonium surface enrichment in Pb by heating [12]. In addition, Lykken described surface emission increasing with elevated sample temperature [13]. Accordingly, an experiment was performed to determine the relative contributions to surface polonium from the atmosphere and internal diffusion.

A 1,075 g mass of tin with emissivity of 2 $\alpha \cdot kh^{-1} \cdot cm^{-2}$ was combined with an 11 g mass of 1,910 $\alpha \cdot kh^{-1} \cdot cm^{-2}$ tin with a significant ^{210}Po surface emission (Fig. 6). The two materials were melted in a graphite crucible and cast into a steel mold to form a 3 × 3 × 35 cm ingot. The ingot was cut in half, and both halves reduced to specific dimensions in preparation for alpha emissivity measurement. One half was used as the test sample, the other half served as a control sample. Both sample and control were measured within two weeks from the initial casting, with respective activities of 23.9 ± 0.8 $\alpha \cdot kh^{-1} \cdot cm^{-2}$ and 22.2 ± 0.9 $\alpha \cdot kh^{-1} \cdot cm^{-2}$. The test sample was oven heated at atmospheric pressure for 6 h at 473K and placed in the ionization chamber within 20 min of removal from the oven. The emissivity was measured, and the control was measured within several days afterward. The test sample was then allowed to sit on clean room wipes on the laboratory bench adjacent to the oven for six hours at 294K, during which time the analyzed surface was face up and exposed to the atmosphere. The test sample was then remeasured, as was the control sample. The measurement/heat/measurement cycle was performed at 15, 45, 46, and 93 days from sample casting to assess the effect of temperature on alpha emissivity and Po distribution. The duration of each heat treatment was 6 h. The samples were stored in sealed polyethylene bags when not being heated or measured.

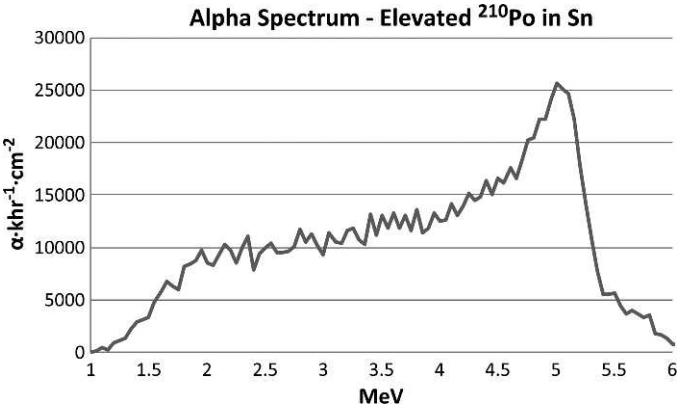

Fig. 6. Alpha emission spectrum from Sn with elevated Po.

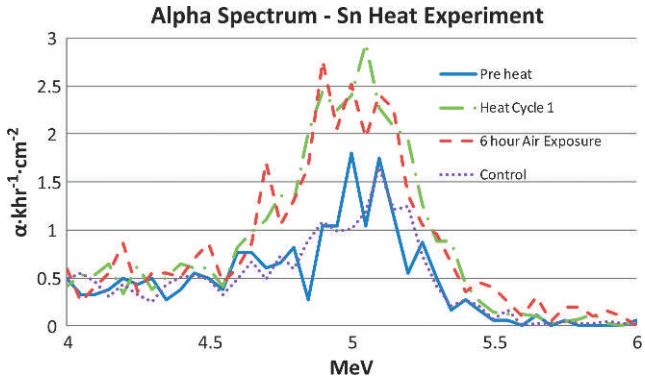

Fig. 7. Normalized alpha spectra for the test sample; (solid line) prior to heat treatment; (dash-dotted line) after first heat cycle; (dashed line) after 6 h air exposure; and (dotted line) the normalized spectrum for the untreated control sample.

The normalized spectra for the test sample before heating, after heating, and after air exposure are shown in Fig. 7, and correspond to the data in Table II for days 9, 15, and 16, respectively. The initial spectrum for both test and control samples are equivalent, and show a significant ^{210}Po peak at 5.3 MeV. After heating, alpha emissivity increased from 23.9 ± 0.8 $\alpha \cdot kh^{-1} \cdot cm^{-2}$ to 32.2 ± 0.7 $\alpha \cdot kh^{-1} \cdot cm^{-2}$, and the integrated ^{210}Po peak intensity from 5.1-5.5 MeV increased from 3.77 counts per hour per channel to 8.03 counts per hour per channel. After the 6 h ambient exposure, the emissivity measured at 33.3 ± 1. The control sample activity was unchanged within measurement uncertainty (22.8 ± 0.7 vs. 22.2 ± 0.9), whereas the test sample increased 38% after heat treatment. The air exposure caused the emission to further increase incrementally, but the change is of the same order as the measurement uncertainty. Comparing the test and control sample results, and considering that polonium diffusion is a function of temperature [13], it is reasonable to conclude that ^{210}Po activity predominately originated from within the sample.

An expression for the polonium concentration in the analytical volume as a function of time may be written as

$$[\mathrm{Po}]_{\mathrm{Surface}}(t) = \frac{\lambda_{\mathrm{Pb}}}{\lambda_{\mathrm{Po}} - \lambda_{\mathrm{Pb}}} \left[^{210}\mathrm{Pb}\right]_0 \left(e^{-\lambda_{\mathrm{Pb}} t} - e^{-\lambda_{\mathrm{Po}} t}\right) + J_{\mathrm{Po}} \quad (3)$$

where λ_{Pb} and λ_{Po} are decay constants and

$$J = -D \frac{\partial \varphi_{\mathrm{Po}}}{\partial x} \quad (4)$$

and where eq. (3) assumes negligible initial Po in the material. The first term reflects the contribution from secular equilibrium, and the second term represents the polonium diffusion contribution. The polonium concentration, and by extension the emissivity, may vary in time depending on which term dominates. Previous work considered only the first term when assessing alpha emissivity versus time [3, 4]. The diffusion term dominates in elevated temperature conditions, while secular equilibrium influence becomes significant when diffusion

Table II
Polonium Diffusion Experimental Data

Test sample				Control sample		
Time elapsed (days)	Heat cycle	Bulk emissivity ($\alpha \cdot kh^{-1} \cdot cm^{-2}$)	^{210}Po emissivity ($\alpha \cdot kh^{-1} \cdot cm^{-2}$)	Time elapsed (days)	Bulk emissivity ($\alpha \cdot kh^{-1} \cdot cm^{-2}$)	^{210}Po emissivity ($\alpha \cdot kh^{-1} \cdot cm^{-2}$)
9		23.9 ± 0.8	4.6	12	22.2 ± 0.8	3.6
15	1	32.2 ± 0.7*	8.6	16	22.8 ± 0.6	4.7
16		33.3 ± 0.9*	8.0	46	26.7 ± 0.9	6.5
45		29.5 ± 0.9	9.3	54	28.2 ± 0.9	7.7
46	2	33.4 ± 1.3*	8.5	92	28.4 ± 1.0	8.8
47	3	33.6 ± 1.1*	9.6	160	33.2 ± 1.0	5.2
92		32.1 ± 1.0	7.1			
93	4	34.2 ± 1.0*	8.5			
163	5	32.5 ± 1.0*	9.7			

*Represents air test data.

slows at room temperature. With respect to eq. (4), diffusion acts to drive the concentration gradient $\partial\varphi/\partial x$ to zero. In the specific case of polonium in tin, diffusion removes the microsegregation-induced concentration gradient and distributes polonium uniformly across the volume.

The total integrated emission from 1-9.5 MeV was plotted versus time in Fig. 8, and the associated data is tabulated in Table II. The preheat measurement of the second test cycle revealed a 13% decrease in the bulk alpha emissivity from 29 d earlier. These data suggest that after initial surface enrichment from elevated temperature diffusion, contributions from secular equilibrium and diffusion at room temperature are insufficient to sustain the surface polonium concentration. The second heat cycle returned alpha flux to the same level measured after the air test. An additional heat cycle 1 d later did not change the emissivity beyond the measurement error. This observation suggests that heating the Sn sample at 473 K for 6 h is sufficient to diffuse polonium uniformly throughout the sample volume, and additional heating yields no additional polonium diffusion. The fourth heat cycle initial measurement is 5% lower than the previous measurement. This suggests a decrease in the number of decays depleting polonium, an increase in polonium from secular equilibrium and diffusion, or a combination of the two. The control sample data in Fig. 8 shows a linear ($R^2 = 0.92$) increase over 160 d at a rate of 7×10^{-5} $\alpha \cdot kh^{-1} \cdot cm^{-2}$ per day. The intersection of the two curves at this juncture indicates that it takes 160 d at room temperature to achieve equivalent diffusion to 6 h at 473K. It should be noted that the grain size and orientation characteristics of the heated sample changed relative to the control sample over the course of the heat treatments. Heat treatment results in significantly different interstitial grain structure between the two samples. As a result, the diffusion mechanisms between the two samples are expected to differ. The difference suggests that both temperature and metallographic texture are significant factors in diffusion processes, and provides a basis to further explore the differential diffusion rates in this system.

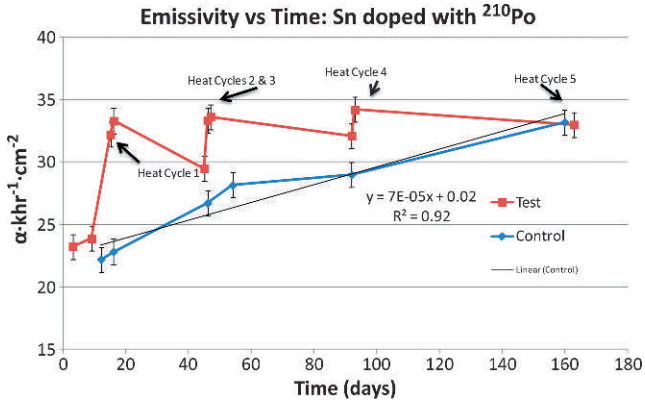

Fig. 8. Alpha emissivity versus time for Sn doped with ^{210}Po.

The surface emission increase of lead sheets was attributed to polonium migration driven by a lower free energy state at the surface relative to the bulk [13]. The data presented above support extending this hypothesis to tin. The surface ^{210}Po emission from Sn solder bumps reported by Gordon [4] could also be explained by this mechanism.

The surface activity was estimated assuming alphas with energies in the interval 5.0-5.6 MeV originated from the sample surface and did not lose appreciable energy in matrix interactions. The range is broad due of the energy resolution limitations of the XIA instrument [11]. The integrated ^{210}Po counts per hour were determined (see Table II), and the number of ^{210}Po atoms N on the surface calculated from

$$N = \frac{At_{1/2}}{\ln 2 f} \tag{5}$$

where $t_{1/2}$ is the half-life of ^{210}Po (3,321 h) and f is the geometric factor from eq. (2). For the first heating cycle, the change in the number of moles on the 1,800 cm^2 tin surface is calculated to be 1.8×10^{-19} mol. Adjusting for sample area and heating time, the ^{210}Po diffusion is calculated to be 4.5×10^{-23} $mol \cdot m^{-2} \cdot s^{-1}$ at 473K. Given that the diffusion occurred over a 6 h period, this is a lower bound on the diffusion rate. Additional experiments utilizing shorter heating intervals will enable more accurate quantification of the diffusion rate. The diffusion rate at 293 K calculated from the control sample data over the test period is 2×10^{-25} $mol \cdot m^{-2} \cdot s^{-1}$. Increasing the temperature 180° increased the diffusion rate by factor of 230.

Packaging Considerations

The implications for packaging applications using tin, tin alloys, or other metal materials are significant. Materials or structures undergoing phase transitions are susceptible to microsegregation, which may lead to incorrect certification to a specified alpha emissivity level because of emitter sequestration outside of the analytical volume. In addition, elevated temperature packaging processes will activate ^{210}Po diffusion to sensitive locations where the 5.3 MeV alpha has a larger cross section of initiating SEU.

The SEU risk from Po is unique and troublesome for two reasons. First, polonium mobility within solid materials has the possibility to negate (to some extent) the shielding effects assumed in IC designs by moving the emitter within range of vulnerable locations. Specifically, diffusion-induced surface emission may cause an unexpected increase in SER if assumptions of volume emission and static emitter position are erroneous [4]. Second, polonium has the combination of high specific activity (alphas emitted per unit mass) and a high energy alpha particle. Therefore, a small number of atoms per unit area will result in a significant high energy alpha flux with an extended range in IC devices.

The secular equilibrium behavior of thin lead samples reported by Gordon [4] show that for processes like electroplating where microsegregation is not present, diffusion effects are minimal and secular equilibrium alone may be sufficient to explain time-dependent alpha emissivity. Microsegregation is not expected in material deposited by processes lacking phase transitions (i.e., electroplating, physical vapor deposition, PVD, or chemical vapor deposition, CVD). However, if contaminants are present in the deposition processes at a sufficient level, it is conceivable that the diffusion mechanism could be active.

The mobility of polonium also requires a fundamental shift in how alpha emissivity is viewed. Alpha emissivity has been assumed to be a volumetric quantity. However, diffusion drives polonium uniformly across the volume, reducing alpha emissivity from a three-dimensional quantity to a two-dimensional quantity. In effect, diffusion increases the emission from a volume where microsegregation is present. The 4π alpha emissivity as a function of sphere diameter was calculated for a hypothetical material with a polonium concentration of 10^4 atoms per gram. The calculations assume 100% polonium diffusion to the surface from an initial homogeneous distribution. This suggests that the alpha emissivity is determined by the absolute, and not relative, number of emitting atoms in the volume. As Fig. 9 indicates, reducing the sphere volume leads to an exponential decrease in alpha emissivity.

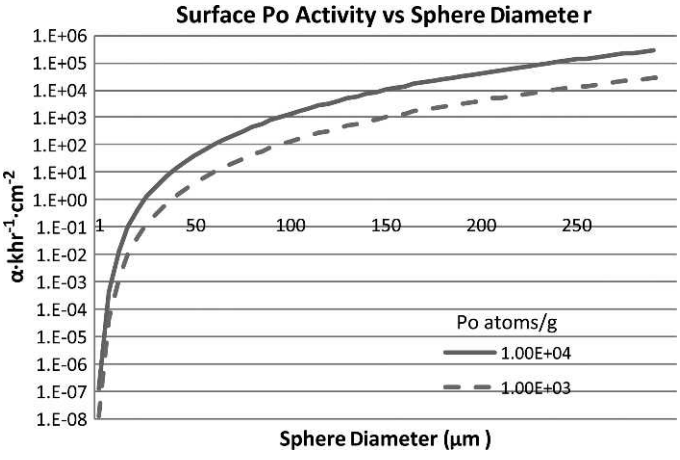

Fig. 9. Sphere surface activity resulting from diffusion of 10^4 atoms Po/g Sn.

While the cautions offered may cause some alarm, it should be noted that examples exist of Sn sufficiently pure that effects from either mechanism are not detectable (sample A of experiment 1). These cases have sufficiently low contaminant concentrations that microsegregation is minimized, and the amount of ^{210}Po is less than measurement limits. The solution is to remove contaminants that are the root cause of the emission, specifically uranium, thorium, and the associated daughters. Refining process capability may be overstated due to microsegregation obscuring true material quality.

Conclusions

The combination of microsegregation and diffusion provide a new basis to explain changes in alpha emissivity of materials. The data suggest that ^{210}Po is a key component in alpha emissivity dynamics. Processing can significantly affect the position of alpha emitters in a material or structure, especially processes that involve liquid/solid phase transitions. The presence of microsegregation on a sub-ppb concentration scale has been reported using direct alpha radiation measurements. In the case of alpha emissivity measurements, the impacts of small analytical volume need to be considered when extrapolating results across the entire volume. Heterogeneity effects on the results can be acute in such circumstances. This emphasizes an inherent limitation involving alpha measurements: analytical volume as a percentage of sample volume is potentially very small. Measurements made assuming near surface volume is representative of the entire sample volume will be erroneous if microsegregation effects are present.

Since nuclear decay is independent of chemical and physical state, any alpha emissivity increase as a function of temperature may be attributed polonium diffusion. A static view of polonium behavior is oversimplified in processes undergoing phase transitions and temperature variations. Transport of ^{210}Po has been quantitatively described, with the rate of diffusion driven by temperature. The dynamic nature of this potential problem underscores the importance of removing these species using specific refining strategies. Data presented demonstrate that material with sufficiently low impurities will be comparably stable over time with respect to alpha emissions.

The data reported confirm earlier published observations of polonium accumulation on the surface of Sn and describe diffusion rates at room and elevated temperatures. The diffusion mechanism can play a significant role in temporal alpha emissivity, and will be amplified to the extent that microsegregation effects are present. Secular equilibrium is expected to explain alpha emissivity in systems where these two mechanisms are absent. Polonium diffusion has been documented in both Sn and Pb.

In cases of polonium diffusion, alpha emission is no longer an intensive property unrelated to the mass of the material. It has been experimentally demonstrated that polonium present

within a mass can be driven to the surface. The amount accumulating at the surface is directly proportional to the absolute amount present in the mass. Therefore, reducing packaging material mass will result in reduced alpha emissions.

Acknowledgments

The author thanks Michael Fields for GDMS analysis and Michael Paladin, Jack Long, and Thomas Ploegman for assistance with sample preparation.

Disclaimer

Although all statements and information contained herein are believed to be accurate and reliable, they are presented without guarantee or warranty of any kind, express or implied. Information provided herein does not relieve the user from the responsibility of carrying out its own tests and experiments, and the user assumes all risks and liability for use of the information and results obtained. Statements or suggestions concerning the use of materials and processes are made without representation or warranty that any such use is free of patent infringement and are not recommendations to infringe any patent. The user should not assume that all toxicity data and safety measures are indicated herein or that other measures may not be required.

References

[1] F. Wrobel, F. Saigne, M. Gedion, J. Gasiot, and R.D. Schrimpf, "Radioactive nuclei induced soft errors at ground level," *IEEE Transactions on Nuclear Science*, Vol. 56, No. 6, pp. 3437-3441, 2009.

[2] D.F. Heidel, K.P. Rodbell, E.H. Cannon, C. Cabral, Jr., M.S. Gordon, P. Oldiges, and H.H.K. Tang, "Alpha-particle-induced upsets in advanced CMOS circuits and technology," *IBM Journal of Research and Development*, Vol. 52, No. 3, pp. 225-232, 2008.

[3] B.M. Clark, M.W. Weiser, and I. Rasiah, "Alpha radiation sources in low alpha materials and implications for low alpha materials refinement," *Thin Solid Films*, Vol. 462, pp. 384-386, 2004.

[4] M.S. Gordon, K.P. Rodbell, D.F. Heidel, C.E. Murray, H.H.K. Tang, B. Dwyer-McNally, and W.K. Warburton, "Alpha particle emission energy spectra from materials used for solder bumps," *IEEE Transactions on Nuclear Science*, Vol. 57, No. 6, pp. 3252-3256, 2010.

[5] F. Wrobel, J. Gasiot, and F. Saigne, "Hafnium and uranium contributions to soft error rate at ground level," *IEEE Transactions on Nuclear Science*, Vol. 55, No. 6, pp. 3141-3145, 2008.

[6] M. Gedion, F. Wrobel, F. Saigne, M. Portier, A.D. Touboul, and R.D. Schrimpf, "Effect of the uranium decay chain disequilibrium on alpha disintegration rate," *IEEE Transactions on Nuclear Science*, Vol. 58, No. 6, pp. 2793-2797, 2011.

[7] JEDEC, "Alpha radiation measurement in electronic materials," *JESD221*, Arlington, VA, http://www.jedec.org/standards-documents.results.jesd221.

[8] J.F. Ziegler, "Particle interactions with matter," http://www.SRIM.org.

[9] H.D. Brody, "Microsegregation," Casting, Vol 15, ASM Handbook, ASM International, 2008, pp. 338-347.

[10] T. Kraft and Y.A. Chang, "Predicting microstructure and microsegregation in multicomponent alloys," *Journal of the Minerals Metals & Materials Society*, Vol. 49, No. 12, pp. 20-28, 1997.

[11] M.S. Gordon, D.F. Heidel, K.P. Rodbell, B. Dwyer-McNally, and W.K. Warburton, "An evaluation of an ultra-low background alpha particle detector," *IEEE Transactions on Nuclear Science*, Vol. 56, No. 6, pp. 3381-3386, 2009.

[12] A. Zastawny, J. Bialon, and T. Sosinski, "Migration of ^{210}Po in lead to the surface," *Applied Radiation and Isotopes*, Vol. 43, No. 9, pp. 1147-1150, 1992.

[13] G. Lykken and B. Momcilovic, "Preparation of Pb thin samples for alpha particle emission test," US patent 6,674,072 January 6, 2004.